

Lithia Porcelains as Promising Breeder Candidates — II. Structural Changes Induced by Fast Neutron Irradiation

Wafa I. Abdel-Fattah,^a Fadel M. Ali^b & R. Abdellah^c

^aNational Research Centre, Ceramic Department, Cairo, Egypt

^bCairo University, Faculty of Science, Biophysics Department, Cairo, Egypt

^cFaculty of Industrial Education, Heliopolis, Cairo, Egypt

(Received 20 November 1995; accepted 9 April 1996)

Abstract: The promise of lithia ceramics as candidate breeder materials necessitates investigations on radiation damage induced structural variations. Prepared porcelain systems consisting of β -eucryptite ($\text{Li}_2\text{O} \cdot \text{Al}_2\text{O}_3 \cdot 2\text{SiO}_2$), its solid-solution ($\text{Li}_2\text{O} \cdot \text{Al}_2\text{O}_3 \cdot 3\text{SiO}_2$) and β -spodumene ($\text{Li}_2\text{O} \cdot \text{Al}_2\text{O}_3 \cdot 4\text{SiO}_2$), previously characterized, were irradiated by fast neutrons at room temperature. A ^{252}Cf source (2 MeV) was used to give fluences of 1×10^5 , 1×10^8 or 1×10^{10} n/cm². Samples of each group received fluences in a one-shot technique, i.e. new samples were used for each fluence before being subjected to structural testing. Damage was assessed by X-ray diffraction (XRD) and infrared (IR) spectral analyses. Relevance dilatation changes were followed through coefficient of change with temperature up to 1000°C. Surface morphologies were examined using scanning electron microscopy (SEM) and selected area electron diffraction (SAED).

XRD patterns revealed various degrees of imperfections that were reflected as shifts in lattice planes. The IR spectral bands suffered shift, especially in the fingerprint region, parallel with the fluence intensity. Coefficient of contraction and/or expansion evidenced various degree of damage, which upon intense irradiation annealed to the original values. SEM micrographs revealed that large grains comprising either β -eucryptite or β -spodumene bodies are much more affected by fast neutrons compared to smaller grains detected in the body containing the solid-solution. Additional evidence was obtained by the SAED results, where the continuous polycrystalline rings of both β -eucryptite and β -spodumene turned upon irradiation to the amorphous metamict state simulating the initial solid-solution structure. The latter acquired higher crystalline order, as well as polycrystalline habit. The degrees of induced imperfections were found to be dependent on initial crystallinity. The higher sensitivity to fast neutrons of β -eucryptite was related to its higher lithia content rather than its hexagonal spiral structure compared to the tetragonal β -spodumene. Intense irradiation caused annealing of the produced damage observed by fragmentation of the grains and various degree of amorphism. © 1997 Elsevier Science Limited and Techna S.r.l.

1 INTRODUCTION

Lithia-bearing compounds, Li_2O , LiAlO_2 , LiSiO_3 and Li_4SiO_4 , were investigated to evaluate the possibilities of breeding in thermonuclear reactor blankets.¹ The International Thermonuclear Experimental Reactor design team (ITER) recognized the promise of lithia ceramics as candidate

breeder materials.² They could also replace coatings on fuel materials, e.g. Al_2O_3 and BeO , which have major problems of cracking during thermal cycling during elevated temperature irradiations.³ Fundamental aspects relevant to radiation damage are the nature and mechanism of the defects created by incident radiation and the extent of alteration in structural and physical properties of

solids. The possible changes in composition and internal structure during service must be primarily considered. Electron diffraction and gas release measurements⁴ of alumina and some other oxide ceramics revealed a quasi-stable amorphous phase after ion bombardment. Amorphism of porcelain minerals was reported.⁵ These induced changes are dependent on the type of solid material itself, its structure and the type of irradiation. Precise and distinguishable quantitative detection of radiation effects on the physical and chemical properties of solids is desirable to define the ultimate range of material performance in intense radiation fields.

In the present work, the effects of low fluences of fission neutrons on the structural and physical properties of lithia–alumina–silica ceramics having different ratios of $\text{Li}_2\text{O}:\text{Al}_2\text{O}_3:\text{SiO}_2$ (LAS) were studied. X-ray diffraction (XRD), infrared (IR) spectral analyses, scanning electron microscopy (SEM) and selected area electron diffraction (SAED) were used to investigate radiation induced structural changes. Thermal expansion changes, being a unique thermophysical property of these ceramics, were used to exemplify physical property changes.

2 EXPERIMENTAL WORK

2.1 Irradiation facilities

Ceramic disk specimens (previously prepared and characterized)⁶ having the chemical composition and the optimum ceramic parameters in Table 1, were prepared at their respective optimum firing temperatures. Disks were irradiated with fission neutrons emitted from a 50 μg ^{252}Cf source with an average energy of 2 MeV. The yield of the source (Radio-chemical Centre, Amersham, England) was between 9×10^7 and 5.8×10^7 n/s.

The source is kept in a cylindrical capsule 0.6 cm diameter and 1.2 cm height, situated in the centre of another cylindrical aluminium container (2.5 cm ϕ and about 4 cm height). Neutron fluences were measured simultaneously at the position of the sample using a calibrated fission track detector type LR-115 (Kodak, Pathe, France). Neutron

irradiations were carried out at room temperature in the centre of a square room of approximately 4 \times 5 m and specimens were fixed in positions to allow for normal incidence of fission neutrons. Six separate fluences (ϕ) in the range 1.1×10^5 up to 1.1×10^{10} n/cm² (i.e. up to 1 Gy) were used to bombard the three lithia-containing bodies, using a one-shot technique, i.e. a new specimen for each neutron exposure.

2.2 Irradiation-induced defects

The structure of the LAS ceramics post-irradiation with each fluence was assessed through X-ray diffraction analysis using $\text{CuK}\alpha$ radiation at $2\theta = 0.25^\circ/\text{min}$. Complementing infrared spectral analysis by the KBr disk technique was used.

Thermal changes were measured for the samples post-irradiation and post-annealing in order to distinguish irradiation-induced effects from those due to heating during measurements.

Morphological changes were studied on the irradiated powders of the finely ground ceramic specimens using scanning electron microscopy (SEM) and selected area electron diffraction (SAED).⁶

3 RESULTS AND DISCUSSION

3.1 X-ray diffraction analysis

The XRD spectra reveal that several peaks suffered broadening with obvious reduction in their relative intensities. A recovery in the line intensities and angle shift were observed upon further irradiation in the intense neutron field. The line shift is indicative of macrostresses, i.e. non-uniform for various planes of the phases.⁷ Maximum shift to lower diffraction angle was attained upon exposure to 1.1×10^{10} n/cm² for β -eucryptite LAS1 (Fig. 1). Its solid-solution LAS2 (Fig. 2) shifted when exposed to both 1.1×10^5 and 1.1×10^{10} n/cm². β -Spodumene samples LAS3 showed merging and broadening of the multiple peaks of 222 hkl plane and lower intensity of the 102 hkl plane with a fluence of 1.1×10^{10} n/cm², denoting partial amorphism (Fig. 3). The response to this high fluence could be attributed to partial changes in both glassy and crystalline phases constituting the body to a common metamict phase.⁸ Such an intermediate phase was reported earlier in quartz and silica glasses upon intense irradiation.⁹

3.2 Infrared analysis

Complete disappearance of certain IR bands in β -eucryptite and its solid-solution (Figs 4 and 5,

Table 1. Chemical composition and optimum ceramic parameters of LAS disks

Notation	Li_2O	Al_2O_3	SiO_2	True density (g/cm ³)	True porosity (%)
LAS1	11.86	40.46	47.68	2.40	8.33
LAS2	9.57	32.67	32.67	2.38	5.46
LAS3	8.03	27.39	27.39	2.68	23.88

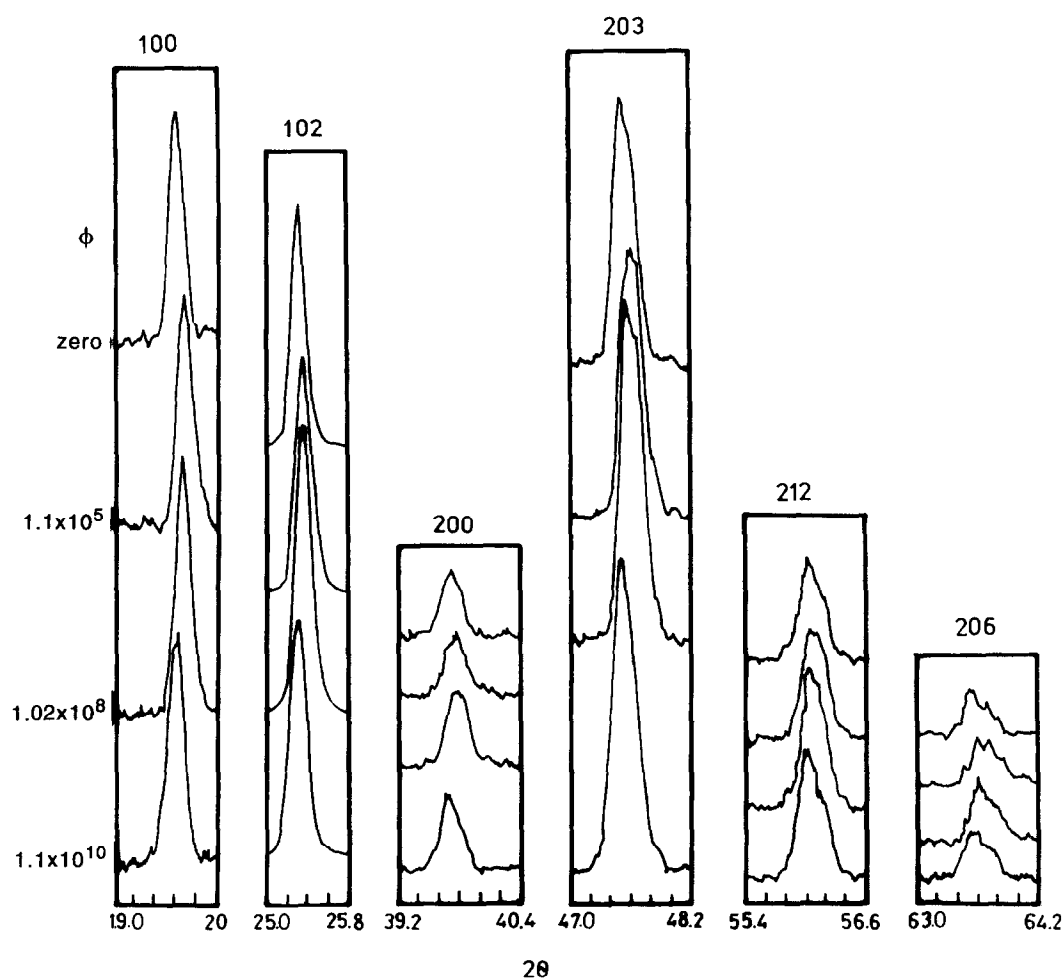


Fig. 1. XRD traces of neutron-irradiated β -eucryptite characteristic planes (LAS1).

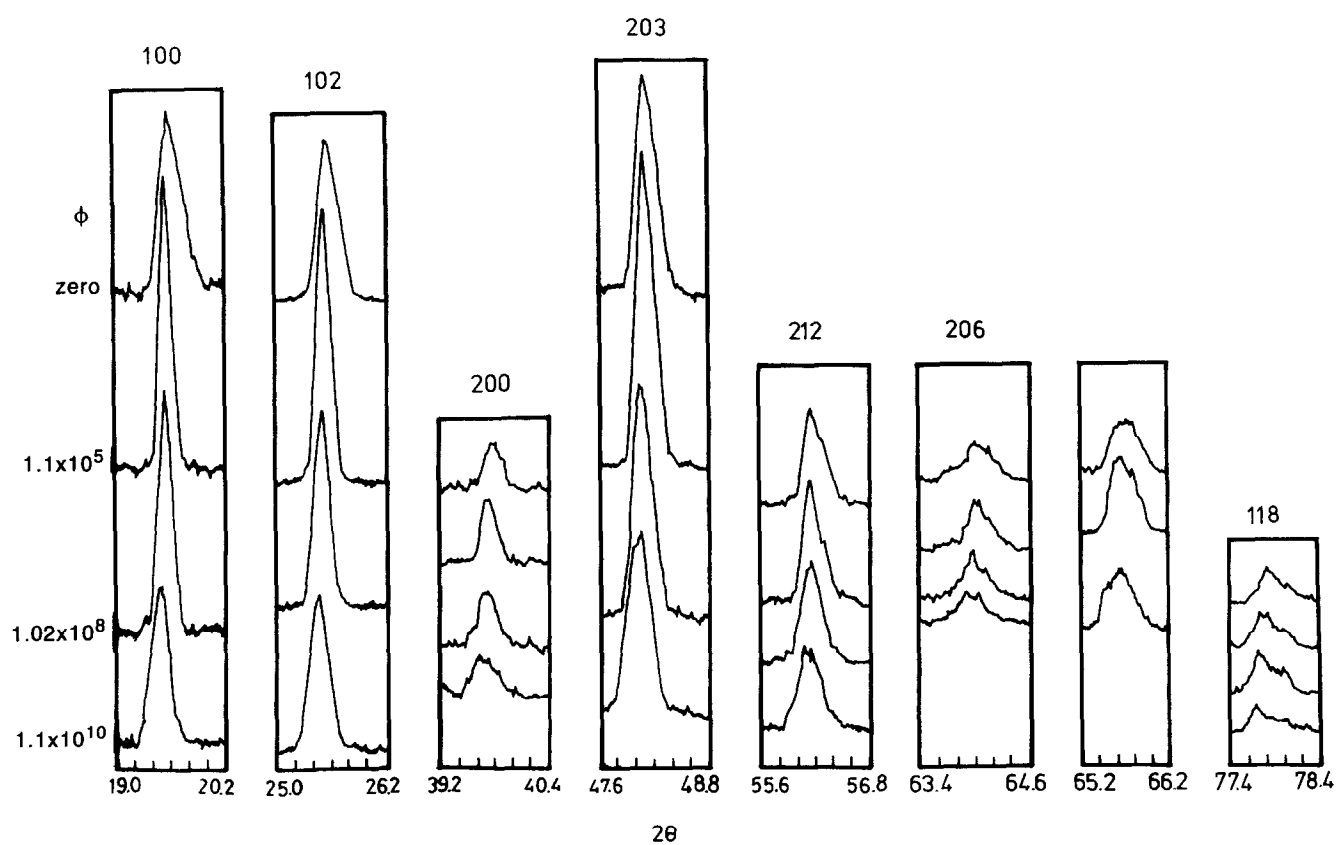


Fig. 2. XRD traces of neutron-irradiated β -eucryptite solid-solution (LAS2).

respectively) denotes their higher sensitivity compared to β -spodumene (Fig. 6), which suffered only some shift in the band positions. Samples partially retained their original structure when subjected to 1.1×10^{10} and 1.02×10^8 n/cm² for the former and latter, respectively. Similar order-disorder transformations were reported for potash and soda feldspar by IR when changing from low to high temperature structure.¹⁰ These changes, being more obvious with higher lithia content, could be explained on the basis that the incoherent scattering of Li is about an order of magnitude larger than the sum of all incoherent cross-sections of other atoms in the formula unit of LiAlSiO₄.¹¹ The broadness of the bands corresponding to water species is related to surface oxidized radiolytic products that are dependent on the neutron irradiation fluence and temperature, as well as the matrix properties of lithium aluminates and lithium silicates.¹² The radiolysis in Li₄SiO₄ and Li₂SiO₃ was assumed to be proportional to the number of Li₂O groups in each.¹³ Also the bands characteristic of water species and those occurring at 12.8 and 13.3 μ m, characteristic of AlO₄⁻, AlO₆⁻ and Si-Al(Si) stretching, suffered diminution in their intensities with a fluence of 1.1×10^5 n/cm². These observations continued with higher fluence (1.1×10^{10} n/cm²), though some bands partially reverted to their original shape. This

reversion occurred at earlier fluences for β -spodumene since the damage was not severe, denoting its lower sensitivity to neutron effects, therefore complementing and confirming the present XRD data.

3.3 Thermal changes

Upon irradiation with 1.1×10^5 n/cm², the negativity of the thermal expansion of all specimens increased (Table 2).

At medium fluence all values increased towards the zero line, approaching the pre-irradiated values. This is explained by the recovery and healing of the irradiation-distorted lattice, as well as the partial release of the accompanying stored energy.¹⁴ The highest experienced fluence (1.1×10^{10} n/cm²) increased the negativity values to approach those induced by the lowest fluence. The zero expansion temperature, T_0 , was attained at higher temperature but without a linear relation with the neutron fluences (Fig. 7). This is attributed to the high concentration of fast neutron-induced vacancies and interstitials, as well as to their accumulation with intense fluence in addition to the energy stored in the lattice due to neutron collisions.¹⁵ The reduced values of expansion are also attributed to the volume expansion resulting from neutron irradiation. Around the path of the neutrons substantial defects in hexagonal minerals

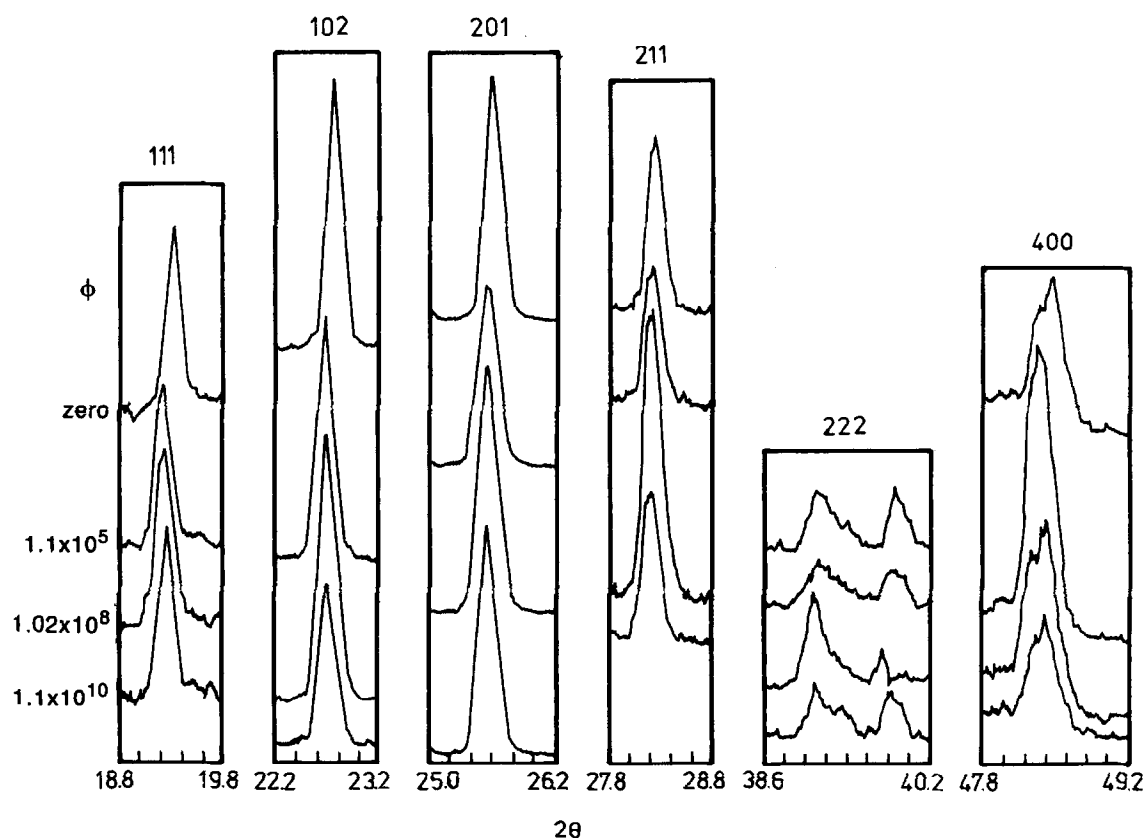


Fig. 3. XRD traces of neutron-irradiated β -spodumene (LAS3).

arise due to the internal stresses.¹⁶ The excessive heating and stored energy are expected to enhance gas movement, migration and outgassing due to

(n, α) reactions¹⁷ contributing to the radiolysis phenomenon known in silicates.¹⁸ The relation between the gradual increase in the silica content of

Table 2. Variation of coefficient of negative (cne) and positive (cpe) thermal expansion ($\times 10^7$) with ϕ

Coefficient Bodies notation Temperature ($^{\circ}\text{C}$) Fluence ϕ	LAS1	cne LAS2 α_{75}^{150}	LAS3	LAS1 α_{350}^{500}	cpe LAS2 α_{450}^{575}	LAS3 α_{500}^{700}
1.1×10^5 *	-17.1	-9.3	-2.1	-50.3	21.6	21.0
1.0×10^6 *	-14.7	-9.3	-4.0	-46.4	25.6	25.5
1.0×10^7	-10.7	-9.3	-2.7	-48.8	24.4	20.5
1.02×10^8 *	-8.0	-6.7	-14.7	-53.6	26.4	23.0
1.03×10^9	-9.3	-6.7	-0.0	-43.2	24.8	—
1.1×10^{10}	-16.0	-8.0	-4.0	-51.2	24.8	14.5
Pre-irradiated	-14.6	-8.0	1.3	-46.4	21.6	24.5

* Maximum effective fluence (n/cm^2).

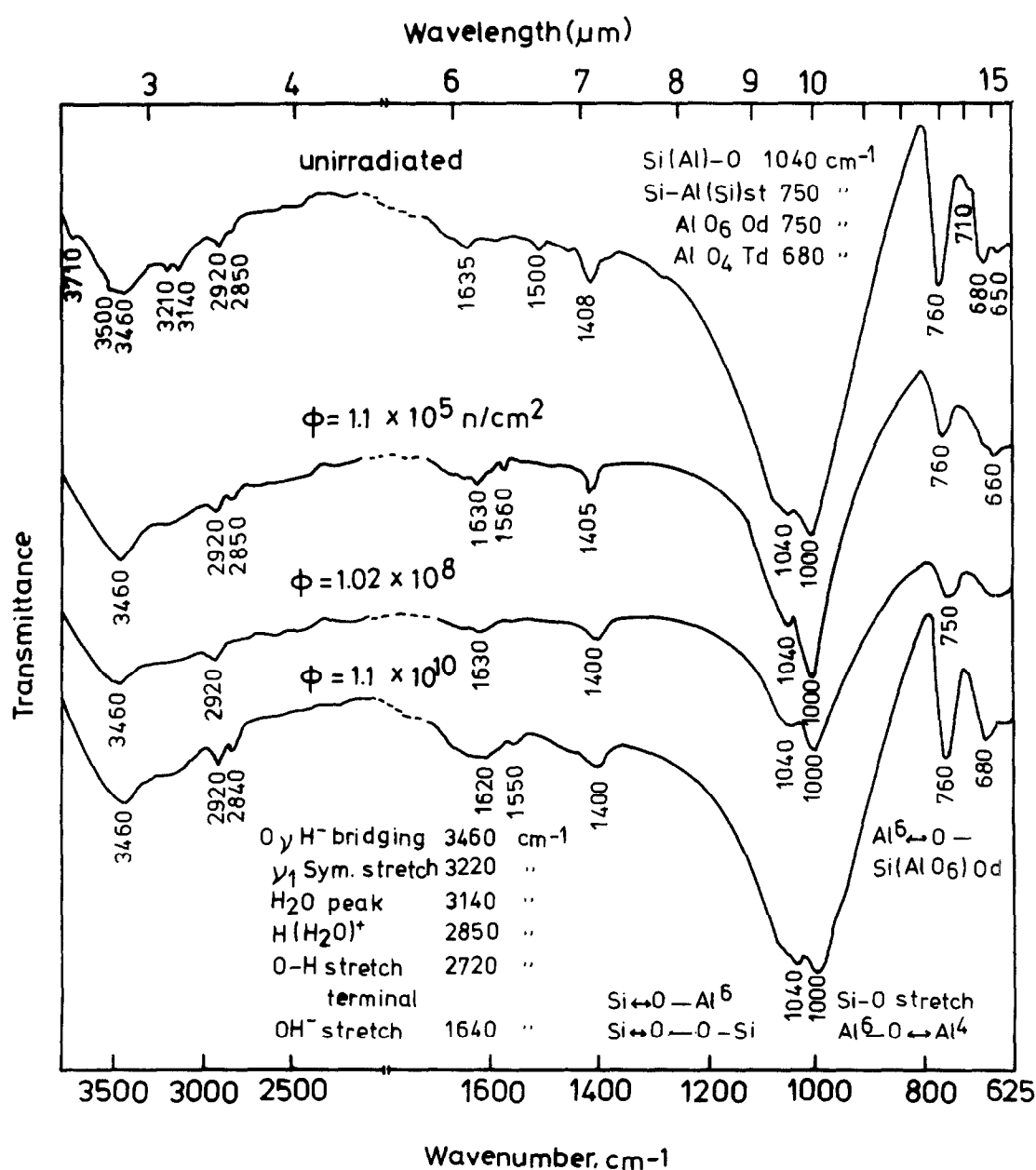


Fig. 4. IR-spectral analysis of β -eucryptite (LAS1) pre- and post-irradiated with fast neutrons.

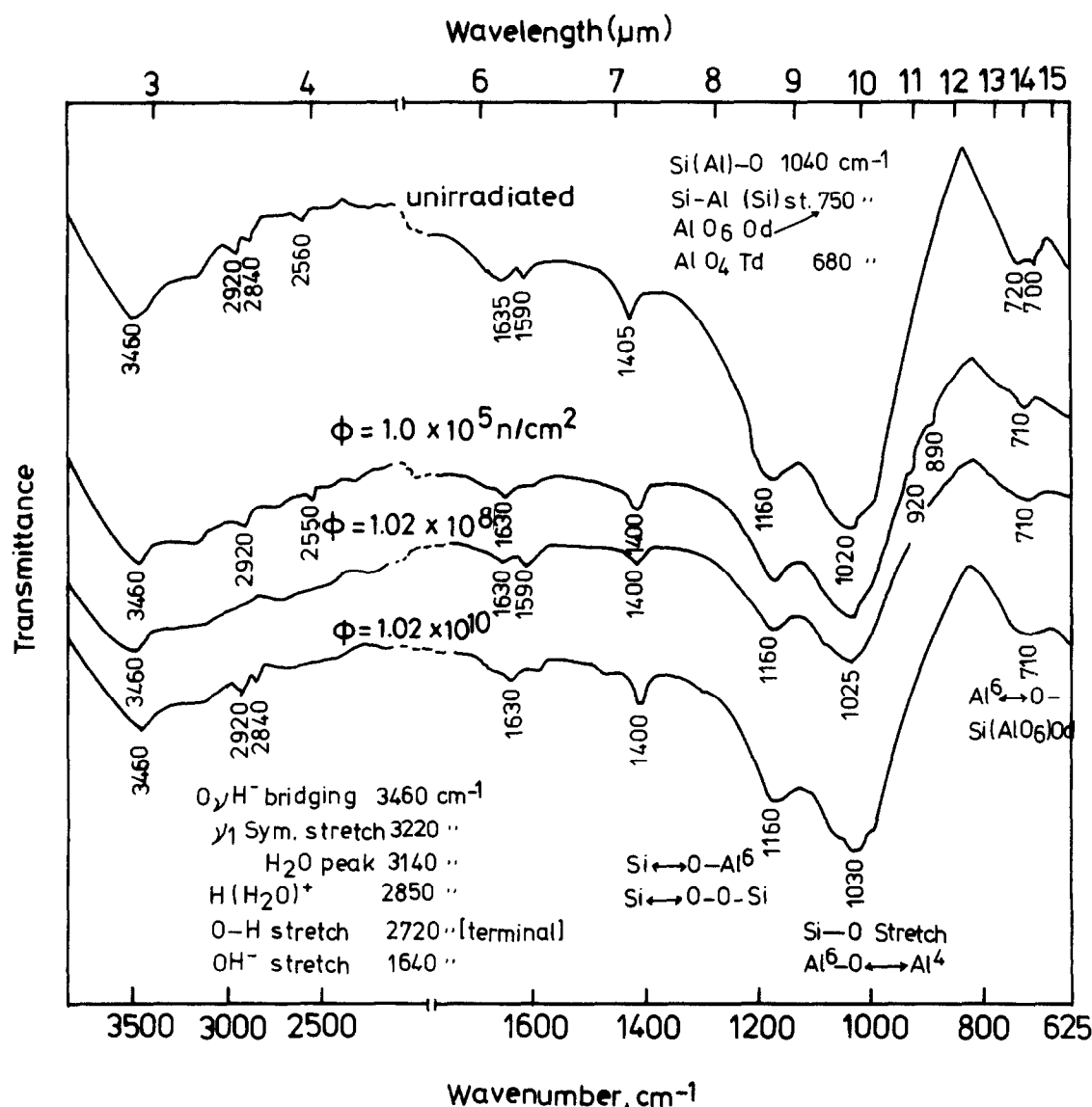


Fig. 6. IR-spectral analysis of β -spodumene solid-solution (LAS3) pre- and post-irradiated with fast neutrons.

4 MORPHOLOGICAL CHANGES

4.1 Scanning electron microscope

The majority of the grains of irradiated β -eucryptite [Fig. 8(a)] are large and opaque. Their grains suffered fragmentation, yielding smaller and finer grains with several areas of contact and undefined morphology, upon irradiation with a fast neutron fluence ($1.1 \times 10^5 \text{ n/cm}^2$). On the other hand, β -eucryptite solid-solution (LAS2) [Fig. 9(a)], upon irradiation with the same fluence, possessed enlarged and well developed crystals with high relief denoting volume expansion or grain growth.²¹ The majority of grains of β -spodumene are also large and opaque, and suffered the same fragmentation as β -eucryptite upon irradiation with a fluence of $1.1 \times 10^5 \text{ n/cm}^2$ [Fig. 10(a)]. A higher fluence of $1.02 \times 10^8 \text{ n/cm}^2$ developed larger areas of contact in both β -eucryptite [Fig. 8(b)] and

its solid-solution [Fig. 9(b)]. This fluence developed enlarged grains having higher relief in β -spodumene [Fig. 10(b)]. This characteristic feature was not obtained for β -eucryptite, even when irradiated to the highest fluence. Great similarity could be seen between specimens of β -eucryptite S.S. and those of β -spodumene irradiated with $1.1 \times 10^{10} \text{ n/cm}^2$ as small grains seemed to be regrouped into larger ones without sharp edges [Fig. 9(c) and Fig. 10(c)]. Those corresponding to β -eucryptite still have structural hexagons beside the grain aggregates.

4.2 Selected area electron diffraction

For β -eucryptite (LAS1) specimens, the disorder is easily demonstrated with a limiting dose higher than $1.0 \times 10^5 \text{ n/cm}^2$, as proved by the faint development of ring patterns. The presence of streaks revealed different types of imperfections, as well as

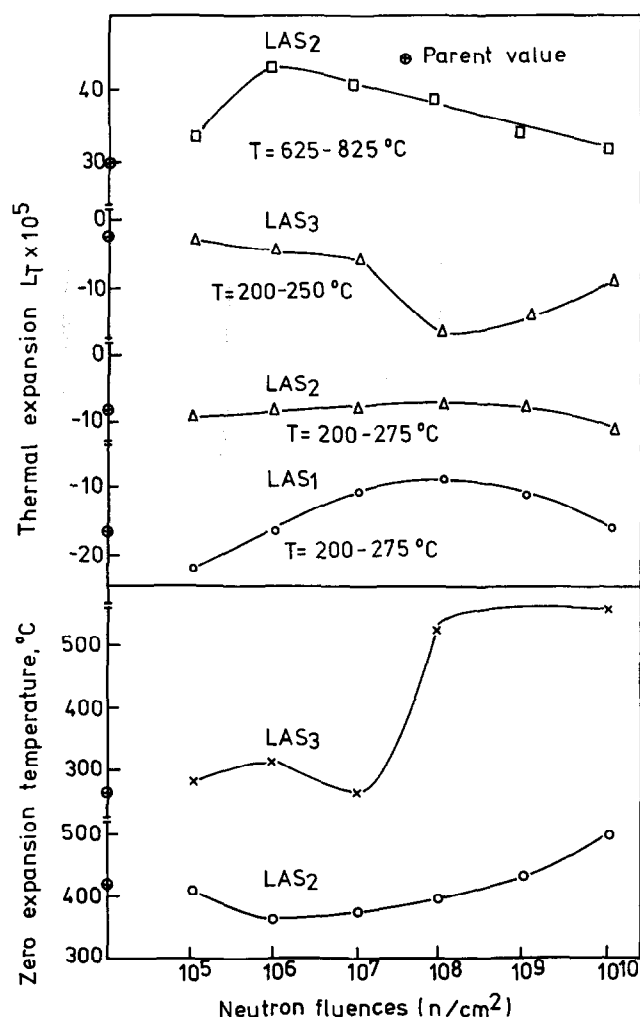


Fig. 7. Variation of L_T at low and high temperature ranges and zero expansion temperature with neutron fluences compared to parent values.

weak crystallinity [Fig. 8(c)]. Additionally, as the central core grew smaller along with the streaks, devitrification in the glassy phase is suspected.²² This common state of crystallinity was previously reported for reactor-irradiated quartz and fused silica.¹⁹ At higher fluence (1.02×10^8 n/cm²) [Fig. 8(d)] a quasi-morphous phase, analogous to that termed by Crawford "radiation-disordered phase", was obtained.²³ The maximum experienced fluence (1.1×10^{10} n/cm²) [Fig. 8(e)] yielded the most defective pattern.

The patterns of β -eucryptite S.S. (LAS2) specimens [Fig. 8(d)] possessed an exceptionally polycrystalline nature with more sharp and continuous rings even than pre-irradiated ones denoting devitrification of the glass when irradiated to the lowest fluence (1.1×10^5 n/cm²). Upon irradiation with a neutron fluence of 1.02×10^8 n/cm², the structure tended to revert its original nature [Fig. 9(e)]. The maximum experienced fluence (1.1×10^{10} n/cm²) also yielded the most defective structure [Fig. 9(f)]. The β -spodumene patterns (LAS3) [Fig. 10(d)]

showed its polycrystalline nature by numerous streaks and spots with faint rings upon irradiation to 1.1×10^5 n/cm², coinciding with volume expansion of the crystals with devitrification of the surrounding glass.²² At higher fluence (1.02×10^8 n/cm²), the rings grew faint with fewer spots [Fig. 10(e)]. This continued with 1.1×10^{10} n/cm² fluence, leading to a larger core denoting more vitrification [Fig. 10(f)]. The higher sensitivity of β -eucryptite to fast neutron irradiation is proved by the ease of formation and subsequent stability of lattice defects under the same given set of radiation conditions.²³

The phenomenon of annihilation of induced damage and reversion to the original condition could be explained by a postulated thermal spike mechanism. The temperature of the area of neutron bombardment is raised up to 1000°C, followed by quenching for a period of less than 10^{-3} s.¹⁵ This might cause the ordering of some crystal planes, relief of certain internal stresses and perhaps some amorphism.⁵ The expansivity of a glass that has been quenched differs from that of the same glass when slowly cooled.²⁴

The neutron fluences ϕ can be expressed as a function of the neutron irradiation induced changes in the thermal contraction measured at 1000°C for β -eucryptite specimens (Fig. 11). The following equation is applied:

$$\Delta L_{Tir} = L_{Tir} - L_{Tp}$$

where L_{Tir} and L_{Tp} are the thermal contraction post- and pre-irradiation, respectively. The plots, when mathematically treated, are found to obey the following semi-empirical formula:

$$\phi = \exp 16.674 \times 10^{-5} - \Delta L / 1.734 \times 10^{-5}$$

Figure 11 shows the values calculated from the equation, along with the experimental values.

5 CONCLUSIONS

The following conclusions can be drawn from the experimental work described above.

- Destruction to both crystalline and amorphous phases was found to be parallel with the increase of the lithium concentration at the expense of silica, denoting higher sensitivity to fast neutron fluence.
- Radiolytic reactions as a result of dissociation of water species are represented as disappearance or reduced intensities of IR-bands. The annihilation phenomenon of

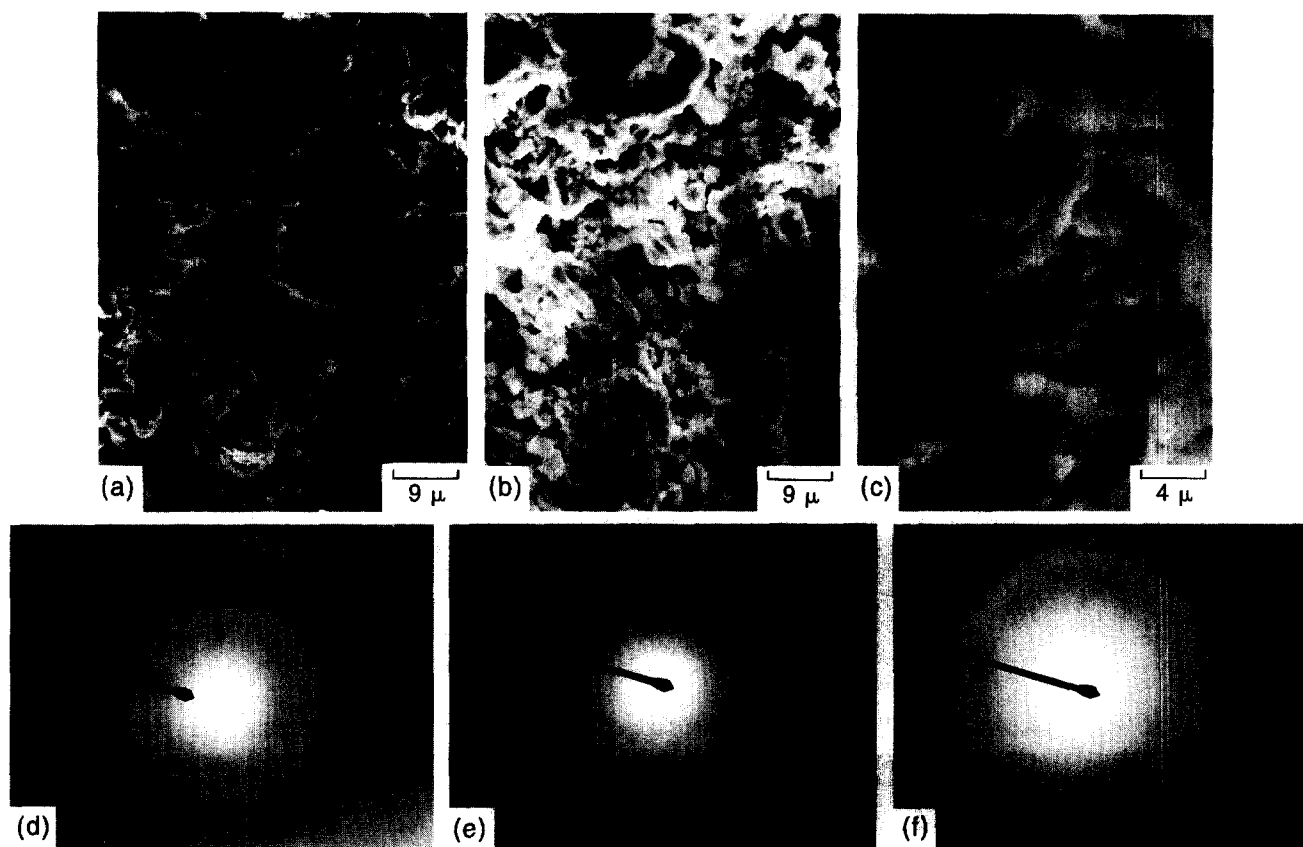


Fig. 8. (a)–(f) SEM of β -eucryptite LAS1 irradiated at $\phi = 10^5$, 10^8 and 10^{10} n/cm², respectively.

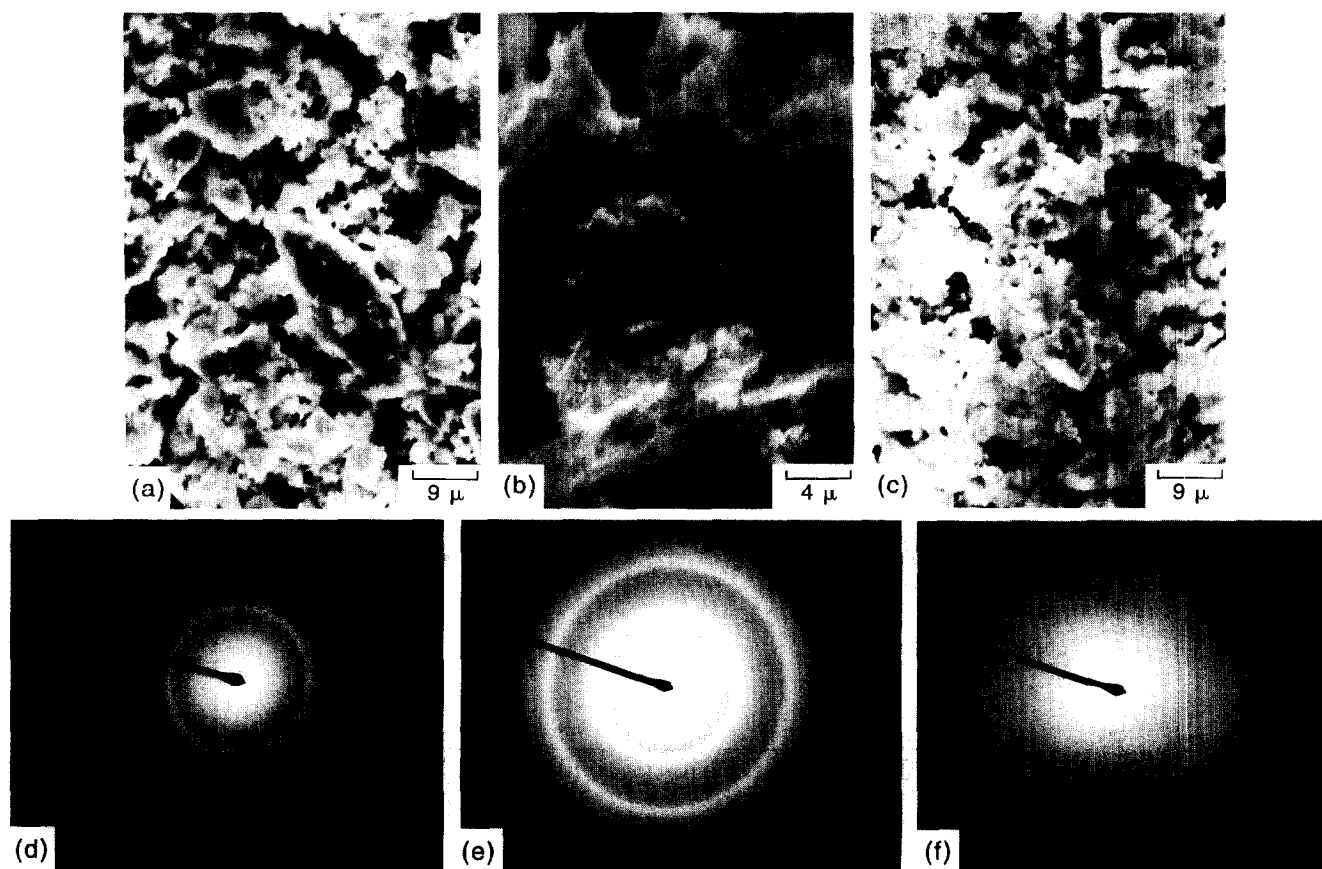


Fig. 9. (a)–(f) SEM of β -eucryptite solid-solution LAS2 irradiated at $\phi = 10^5$, 10^8 and 10^{10} n/cm², respectively.

damage with intense fluences was proved by reappearance of some silicate bands.

- The retarded zero-expansions with higher fluence are related to stored energy beside lithium hopping and consequent lattice defects.

Maximum effective fluence was composition dependent.

- Low fluences resulted in large crystallite size, and sharp rings of β -eucryptite and β -spodumene changed to smaller ones with faint rings

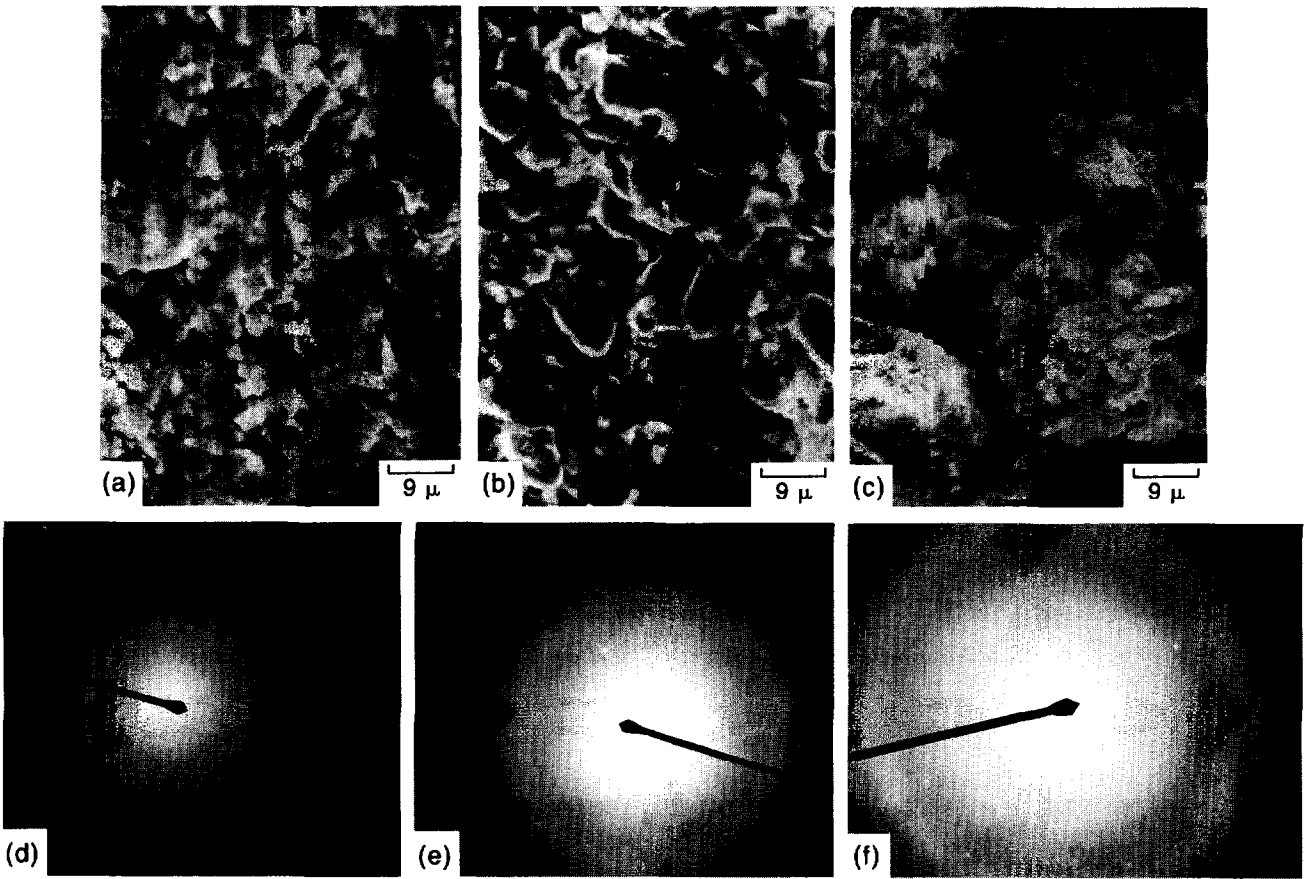


Fig. 10. (a)–(f) SEM of β -spodumene LAS3 irradiated at $\phi = 10^5$, 10^8 and 10^{10} n/cm², respectively.

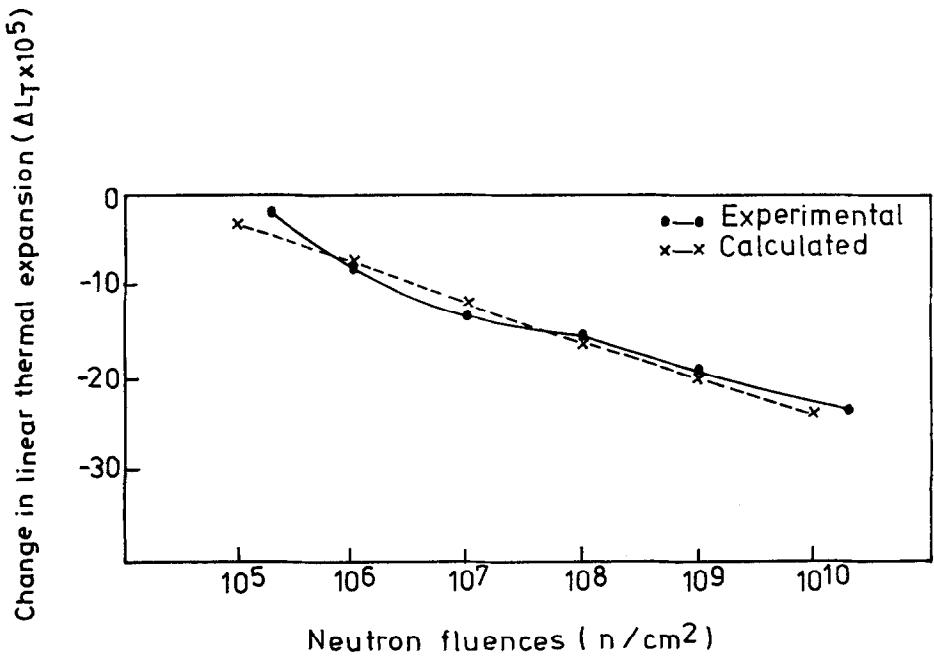


Fig. 11. Variation of ΔL_T measured at 1000°C for β -eucryptite LAS1 as a function of neutron fluence considering non-irradiated specimens as a base.

and streaks. The reverse occurred for β -eucryptite solid-solution. At higher neutron fluences, expansion of the small crystallites and fragmentation of large ones were coupled with faint rings and glass devitrification. Signs of defect saturation and partial annihilation were also noted.

- A convenient semi-empirical formula was derived for calculating neutron fluences as a function of the variation in the negative thermal expansion for β -eucryptite (LAS1).
- β -Eucryptite LAS2 solid-solution is preferable as a breeder for its intermediate characteristics, high lithium oxide content and reasonable thermal expansion coefficient.

REFERENCES

1. VASILEV, V. G., BORISOV, S. R., RYAZANTSEVA N. N. & VASHMAN A. A., *Russian Atomic Energy*, **48**(6) (1982) 392; C/O *Chem. Abstr.* 93 (1980) 15 7216t.
2. JOHNSON, C. E., In *7th Cimtec Word Ceramic Congress, Ceramics Today Tomorrow's Ceramics*. Montcatini, 24–30 June 1990, B.5. 2-LO1.
3. TOWNLEY, C. W., MILLER, N. E., RILZMAN, R. H. & CURIAN, R. J., *Nucleonics*, **22**(2) (1964) 43.
4. MATZKE, H. & WHITTON, J. L., *Can. J. Phys.*, **44** (1966) 995.
5. ABDEL-FATTAH, W. I., ABOU-SAIF, E. A. & AL-ALOUSI, D. S., *Sprechsaal*, **10** (1981) 753.
6. ABDEL-FATTAH, W. I. & ABDELLAH, R., *Ceram. Int.*, this volume.
7. CULLITY, B. D., *Elements of X-Ray Diffraction*. Addison Wesley Pub. Co. Inc., Reading, MA, USA, 1987, pp. 81–88.
8. COHEN, A. F., *J. Appl. Phys.*, **29** (1958) 591.
9. HOLLAND, H. D. & KULP, J. L., *Science*, **111** (1950) B12.
10. SMITH, J. V., *Feldspar Minerals (Crystal Structure and Physical Properties)*, Vol. 1. Springer Verlag, Berlin, 1974.
11. SCHULZ, H. J., PRESS, W., PENKER, B. & BOHM, H., *Phys. Rev. B*, **21**(3) (1980) 1250.
12. HALMEIER, K., DZALME, J., KIZANE, G. & TILIKS, Letv. PSR. Zinat. Akad., Vestis, Fiz. Tech. Zinat. Ser (2) 7–10. C/O *Chem. Abstr.* 1062 (1984) 14903n report.
13. PRONIN, I. S., WASHMAN, A. A. & NIKIFOROV, A. S., *Russian Atomic Energy*, **59**(3) (1985) 227; *Chem. Abstr.* 103(26) (1985) 222649C.
14. NELSON, R. S., *J. Nucl. Mol.*, **88** (1980) 23, 322.
15. KREIDL, N. J., *Ceramics in Serve Environments*, Vol. 5. Plenum Press, NY, 1971.
16. BERGGREN, G., Thermal analysis. In *Proc. 4th ICTA*, Vol. 3. Budapest, 1974, pp. 41–42.
17. ERDMANN, G., *Kernchemi in Einzeldarstellugen* 6. Weinheim, Verlagchemi, Weinheim, New York, 1976.
18. HOBBS, L. W. & PAXCUCCI, M. R., *J. Phys. Collag.*, **6** (1980) 237.
19. CHILDS, B. G., *J. Nucl. Mater.*, **5** (1962) 28.
20. ABDEL-FATTAH, W. I., RAMADAN, A. A., EL-SHAABINI, A., ABDELLAH, R. & FADEL, M. A., *Rad. Phys. Chem.*, **40**(3) (1992) 181.
21. HURLEY, G. F. & BUNCH, J. M., *Bull. Am. Ceram. Soc.*, **59**(4) (1980) 436.
22. HOWIE, J., *J. Nucl. Eng.*, **62**(6) (1961) 299.
23. CRAWFORD, J. H. & BULL, J. R., *J. Am. Ceram. Soc.*, **44**(12) (1955) 963.
24. RITLAND, N. H., *J. Am. Ceram. Soc.*, **39** (1956) 403.